EXPERIMENTAL AND THEORETICAL LEVEL DENSITIES[1]

ANDRZEJ MARCINKOWSKI*, Warsaw

First, we shall discuss different methods for experimental determination of level densities which are based mostly on analytical level density formulae. In the second part, more refined, microscopic approaches to level densities will be described.

I. INTRODUCTION

Measurements of the nuclear level density provide information about the structure of highly excited nuclei and allow us to understand and analyze the decay of the compound nuclei formed in complex nuclear reactions.

II. EXPERIMENTAL AND THEORETICAL ASPECTS OF THE PROBLEM

Most of the experimental data concerning level densities have been obtained using indirect methods based on theoretical, analytical expressions for nuclear level density. Traditionally the equidistant model in which the single particle levels are equally spaced and nondegenerate has been in the evaluation and analysis of experimental data. The density of levels of a given spin value I of a system of independent fermions with an equidistant single particle level spectrum is given by the known Bethe formula [1, 2]

$$\varrho(U, J) = \frac{\omega(U)}{\sqrt{2\pi\sigma^2}} \frac{2J+1}{2\sigma^2} \exp\left[-\frac{J(J+1)}{2\sigma^2}\right] \tag{1}$$

with the state density

$$\omega(U) = \frac{\sqrt{\pi} \exp 2\sqrt{a(U-\Delta)}}{12a^{1/4}(U+t-\Delta)^{5/4}}. \tag{2}$$

* Insititute of Nuclear Research, Hoża 69, 00681 WARSAW, Poland.

[1] Lecture given at the International Symposium on Neutron Induced Reactions, September 2—6, 1974 at SMOLENICE, Czechoslovakia.

In the formulae a, σ^2, U, t and Δ are the Fermi-gas level density parameter, the spin cut-off parameter, the excitation energy, the thermodynamic temperature and the energy shift parameter, respectively.

The constant temperature level density

$$\varrho(U, J) = const \frac{\varrho(U)}{2\sigma^2} \exp\left[-\frac{J(J+1)}{2\sigma^2}\right] \tag{3}$$

with

$$\varrho(U) = \text{const}' \exp\left(\frac{U-\Delta}{T}\right), \tag{4}$$

where t is the nuclear temperature, has also been often used in the analysis of experimental data mainly because of its simplicity.

The most extensive information about the level densities has been obtained by counting the resolved slow neutron resonances corresponding to a narrow excitation energy range near the neutron binding energy. In this way the average level spacing for almost 200 nuclei have been determined [3]. Compilations of the a parameter values obtained from neutron resonance data analysis [4, 5] show that a increases with the mass number A of the nucleus like $A/8$ with marked deviations from the smooth trend especially in the vicinity of closed shells.

Similar information may be obtained from the charged particle capture resonances as well as from the fine structure resonances of the analogue states, studied by means of the proton elastic scattering [6, 7]. In all such measurements one always worries whether the resonances observed are truly representative of the total level density, because the nuclear structure may introduce fluctuations of the number of levels observed and this may in turn lead to a sizable error.

The level density parameters have for a long time been also determine from particle evaporation spectra. Usualy the spectra have been analysed with the approximate Weisskopf expression

$$I(\varepsilon_b)\, \mathrm{d}\varepsilon_b = const\ \varepsilon_b \sigma(\varepsilon_b) \omega(U)\, \mathrm{d}\varepsilon_b, \tag{5}$$

which relates the spectral intensity of the evaporated particles $I(\varepsilon_b)$ with the inverse cross section $\sigma(\varepsilon_b)$ and the energy ε_b of the emitted particle. Substituting into Eq. (5) the state density (2) one can determine the a parameter from the slope of the quantity $\ln\{I(\varepsilon_b)\,(U+t-\Delta)^n/\varepsilon_b\sigma(\varepsilon_b)\}$ as a function of $(U-\Delta)^{1/2}$. Here n is the power determining the energy dependence of the preexponential term of the level density. It is equal to 5/4 for the state density given by Eq. (2). The evaporation spectra have been analysed in the literature with different n values ranging from 0 to 2.

The inclusion of angular momentum effects in compound nucleus reactions leads to an exact angular and energy dependent differential cross given by the Blatt and Biedenharn formula [8]

$$\frac{\mathrm{d}^2\sigma}{\mathrm{d}\varepsilon_b\, \mathrm{d}\Omega} = \sum_{L=0}^{\infty} B_L(\varepsilon_b)\, P_L(\cos\Theta) \tag{6}$$

$$B_L(\varepsilon_b) = \frac{K_a^{-2}}{4(2I_a+1)(2s_a+1)} \sum_{S_a, l_a, J, I_b, l_b, S_b} \frac{(-)^{S_a-S_b}}{G(J)} T_{l_a} T_{l_b} Z_a Z_b \times \varrho(U_b, I_b) \tag{7}$$

and $G(J)$ is given by

$$G(J) = \sum_{b'} \int \mathrm{d}U_{b'} \sum_{I_{b'}} \sum_{S_{b'}=|I_{b'}-s_{b'}|}^{I_{b'}+s_{b'}} \sum_{l_{b'}=|J-S_{b'}|}^{J+S_{b'}} T_{l_{b'}} \varrho(U_{b'}, I_{b'})\,. \tag{8}$$

The quantities I_a, i_a, J, I_b and i_b are the spins of the target, the projectile, the compound nucleus, the residual nucleus and the emitted particle, respectively; S_a and S_b are the entrance and the exit channel spins; l_a and l_b are the orbital angular momenta of the projectile and the emitted particle, respectively; K_a is the wave number of the projectile; $P_L(\cos\Theta)$ is the Legendre polynomial; T_{l_a}, T_{l_b} are the transmission coefficients and ε_a, ε_b the channel energies of the projectile and the emitted particle, respectively. Z_a, Z_b are the Z-coefficients expressed by the Racah and Clebsch-Gordan coefficients.

The fit of the theoretical spectra calculated with the help of Eqs. (6—8) to the experimental evaporation spectra provides more accurate level density parameters. The theoretical spectra obtained from such a fit were analysed by Lu et al. [9] with the use of the conventional slope method. This analysis demonstrates the degree of variation of a values obtained from the slope method with the different factors contained in Eq. (5). It has been calculated that the conventional analysis of spectra with the Weisskopf like expression gives the Fermi gas level density parameter a which depends on the reaction studied. The correct value of the a parameter may be derived with the slope method by an adjustment of the value of n. The value of a increases with an increasing n, Fig. 1. Usually each different reaction requires a different value of n.

Another method of level density determination was proposed by Ericson [10], who pointed out that absolute cross sections for the formation of isolated residual levels in compound nucleus reactions depended on the level densities of various residual nuclei formed in the interaction between a particular projectile and the target. Usually only the residual nuclei formed by the emission of neutrons, protons and α-particles need to be considered and the level

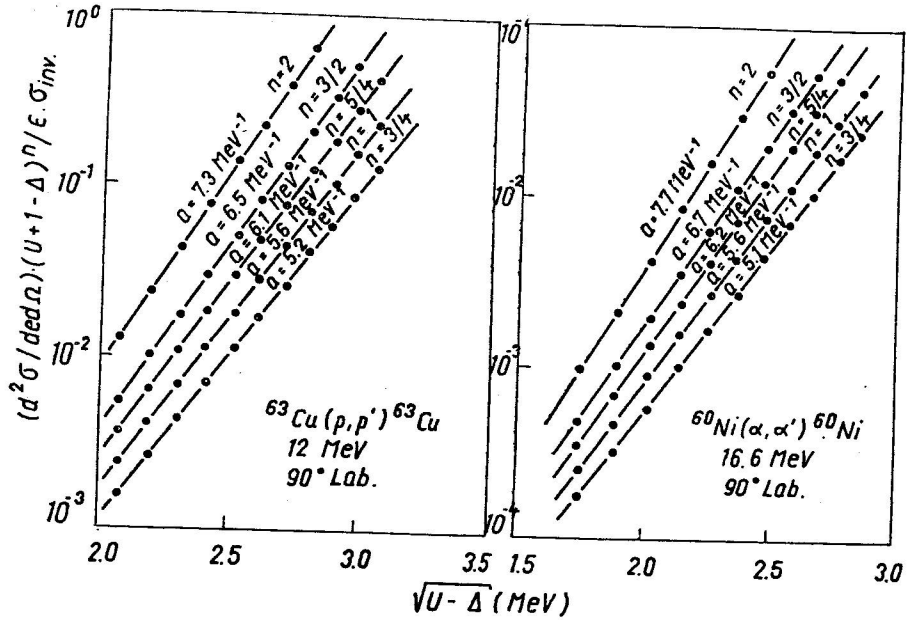

Fig. 1. Dependence of the Fermi-gas level density parameter a on the power n which determines the energy dependence of the preexponential term of the level density. The input values of a used in the calculation of the theoretical spectra were 6.8 MeV^{-1} for ^{63}Cu and 5.8 MeV^{-1} for ^{60}Ni. The figure is taken from Ref. [9].

densities of the three residual nuclei can be determined from the cross section of isolated levels. The applicability of this method to level density measurements was demonstrated by Huizenga et al. [11]. These authors have used the (p, α) and (α, p) reactions for the determination of the level density parameters. It was found that the back-shifted Fermi gas model [12, 13], in which the energy shift Δ is treated as an adjustable parameter accounting for both the pairing and the shell structure, could be brought into a good agreement with the experiment, Fig. 2, whereas the conventional shifted Fermi gas with Δ equal to the pairing energy shifts underestimates the level density at a low excitation energy giving thus an uncorrect slope of the excitation curves.

The absolute cross section for isolated levels can be used in conjunction with the known level width Γ_{fl} obtained from cross section fluctuation measurements to determine level densities of compound nuclei [11, 14]. This method allows to estimate the level density at excitation energies near to 20 MeV. It is based upon the fact that the denominator in the exact differential cross section formula Eq. (8) is simply related to the total width of a compound state $\Gamma_{J\pi}$ and the spacing of the levels $D_{J\pi}$ width spin I and the parity

$$\Gamma_{J\pi} = \frac{D_{J\pi}}{2\pi} G(J) . \tag{9}$$

Substituting Eq. (9) into (6) for an isolated level with the spin I_b and the parity π_b, and replacing $\Gamma_{J\pi}$ by an average value Γ which may be removed from the summation over I one obtains

$$\frac{\mathrm{d}\sigma}{\mathrm{d}\Omega}(U_b, I_b, \pi_b, \Theta)\frac{\Gamma(U_c)}{D_{o\pi}} = \\ = \frac{K_a^{-2}}{8\pi(2I_a+1)(2s_a+1)} \sum_{S_a,l_a,J,I_b,l_b,S_b} \frac{(-1)^{S_a-S_b} T_{l_a} T_{l_b} Z_a Z_b P_L(\cos\Theta)}{(2J+1)\exp[-J(J+1)/2\sigma_c^2]} \tag{10}$$

where σ_c^2 is the spin cutoff factor of the compound nucleus at the excitation energy U_c. By assuming $\Gamma = \Gamma_{fl}$ information about $D_{o\pi}$ can be obtained from Eq. (10) if $\mathrm{d}\sigma/\mathrm{d}\Omega$ is measured. The averaging procedures applied to obtained Γ and Γ_{fl} are not exactly the same, but as was discussed by Huizenga et al. [11] the differences are small compared to the experimental errors in Γ_{fl}. The resulting compound nucleus level densities are again fitted best by the back-shifted Fermi gas level density which reproduces well the low and the high-excitation energy data [11].

The preference of the back-shifted model finds its justifications of Bloch [15] and Rosenzweig [16]. These authors have shown that when the degen-

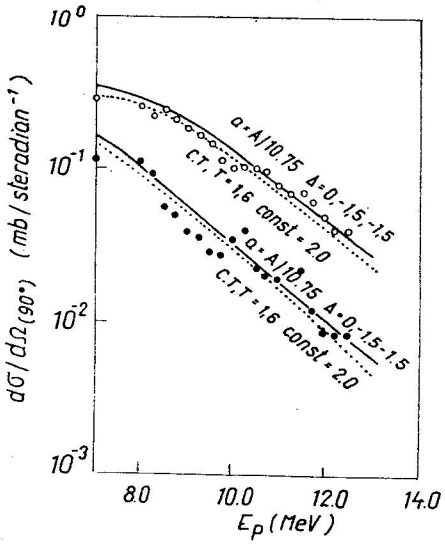

Fig. 2. Differential cross-section at 90° as a function of the proton bombarding energy for the ^{55}Mn (p, α_0) ^{52}Cr and ^{55}Mn (p, α_1) ^{52}Cr reactions. The lines are theoretical calculations with various level density parameters. The energy shifts are given for residual nuclei formed by α, proton and neutron emission, respectively. The dotted lines are constant temperature calculations. The figure is taken from Ref. [11].

eracy of the single particle levels is accounted for, the level density is still described approximately by the Fermi gas model with an additional shift of its ground state. For nuclei far from closed shells this shift is about the same magnitude as and opposite in sign to the pairing energy shift. Neither of these shifts can be calculated accurately. The total shift can be obtained by matching the known experimental data with the Fermi gas algebraic formulae. However, these formulae contain approximations of purely mathematical nature and their shortcomings for matching experimental data are overcome by parameter adjustment. The directness of the confrontation of theoretical models with level density data suffers in consequence.

III. MICROSCOPIC APPROACH TO LEVEL DENSITIES

In order to improve the methods for exploring the structure of highly excited nuclei through their level densities and avoid the numerous approximations some authors calculated level densities numerically [17—19]. Hillman and Grover [17] generated a large set of configurations representing the ground state and many excited states, by permutation of all the nucleons among the single particle levels of the shell model. The energies of the configurations corrected for pairing were calculated by the *BCS* method. The calculations were restricted to spherical nuclei for which the orbital spin becomes a good quantum number. The number of levels of a given total angular momentum I for a particular configuration of subshells was calculated by finding the number of ways in which the components j can couple to J. The comparison of the results of numerical calculations with those obtained from the analytical formula (1) is given in Fig. 3. It is interesting to note that

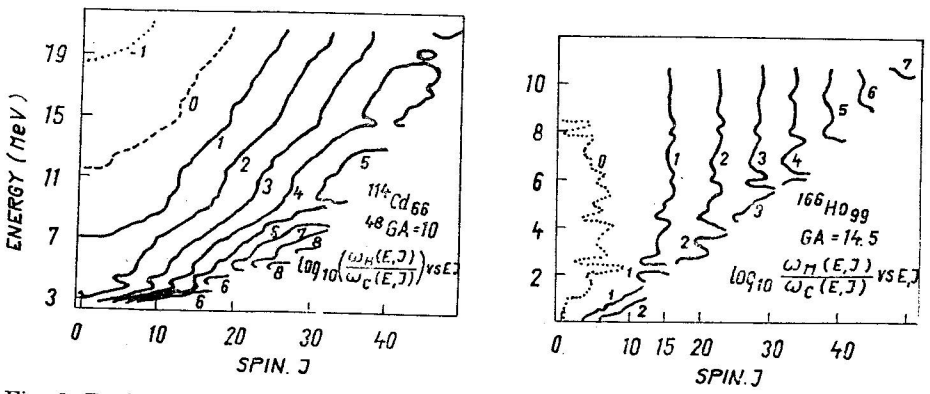

Fig. 3. Ratio of level densities calculated numerically to those calculated by analytical formula. The figure is taken from Ref. [17].

there is almost no energy dependence of the ratio of level density calculated numerically to that calculated from the analytical formula for ^{166}Ho, which is far from the closed shell, whereas for ^{114}Cd marked discrepancies occur for both energy and spin dependence. This comparison was made to reveal the shortcomings of the algebraic formulation. Some of these shortcoming may be overcome by application of realistic sets of single particle levels in level density calculations. The use of single particle levels obtained from a shell model in the evaluation of level density by the grand partition function method was initiated by Sano and Yamazaki [20]. In order to obtain a meaningful comparison between theory and experiment the residual pairing interaction was introduced and the *BCS* formalism of the superconductivity theory was applied to obtain the Hamiltonian describing a system of paired fermions.

This Hamiltonian is approximately diagonalized by means of a transformation where the quasiparticle excitations are considered to be independent fermions with the energy $E_k = [(\varepsilon_k - \lambda)^2 + \Delta^2]^{1/2}$. Here λ is the chemical potential, ε_k are the single particle energies and Δ is the energy gap parameter.

For the paired system of one type nucleons the logarithm of the grand partition function Z, obtained as a trace of the Hamiltonian is

$$\ln Z = -\beta \sum_k (\varepsilon_k - \lambda - E_k) + 2 \sum_k \ln [1 + \exp(-\beta E_k)] - \frac{\beta \Delta^2}{G} \qquad (11)$$

where G is the pairing strength and β is the reciprocal of the temperature t. The summation runs over doubly degenerate orbitals k. The variables Δ, λ, β satisfy the gap equation

$$\frac{2}{G} = \sum_k \frac{\tanh(1/2\beta E_k)}{E_k}. \qquad (12)$$

The state density is given by the inverse Laplace transform of the grand partition function [10]. Using the saddle point method to evaluate it we obtain

$$\omega = \frac{\exp S}{(2\pi)^{\frac{1}{2}n} D^{\frac{1}{2}}}, \qquad (13)$$

where n is the number of constants of motion describing the state of the system. In the case of a definite energy E and the number of nucleons N the entropy S is given by

$$S = \ln Z - \beta E + \beta \lambda N \qquad (14)$$

and

$$D = \det \frac{\partial^2 \ln Z}{\partial\beta\partial\beta\lambda}. \tag{15}$$

In Eq. (13) both S and D should be evaluated for the saddle point values of the Lagrange multipliers β and $\beta\lambda$. These values are defined by

$$\frac{\partial S}{\partial \beta} = 0; \quad \frac{\partial S}{\partial \beta\lambda} = 0. \tag{16}$$

Differentiating the grand particion function given by Eq. (11) and satisfying Eq. (16) one finds the number of nucleons N and the energy of the system E

$$N = \sum_k \left[1 - \frac{\varepsilon_k - \lambda}{E_k} \tanh\left(\tfrac{1}{2}\beta E_k\right)\right], \tag{17}$$

$$E = \sum_k \varepsilon_k \left[1 - \frac{\varepsilon_k - \lambda}{E_k} \tanh\left(\tfrac{1}{2}\beta E_k\right)\right] - \frac{\Delta^2}{G}.$$

Also the spin cut-off parameter σ^2 can be expressed in terms of the variables used [22]

$$\sigma^2 = \tfrac{1}{2} \sum_k m_k^2 \operatorname{sech}^2\left(\tfrac{1}{2}\beta E_k\right). \tag{18}$$

For the entire nucleons we make use of the additive properties of the following magnitudes

$$\ln Z = \ln Z_p + \ln Z_n \tag{19}$$

$$E = E_p + E_n$$

$$S = S_p + S_n$$

$$\sigma^2 = \sigma_p^2 + \sigma_n^2$$

here p and n refer to protons and neutrons, respectively. The above expressions allow to calculate the level density

$$\varrho(U, N_p, N_n) = \omega(U, N_p, N_n)/(2\pi\sigma^2)^{1/2} \tag{20}$$

with the excitation energy given by

$$U = E(t) - E(0). \tag{21}$$

The model described above was used by Decowski et al. [21, 22] in the calculations of excitation curves for a variety of neutron induced reactions.

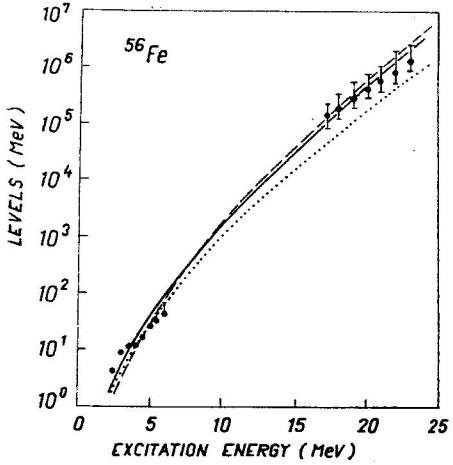

Fig. 4. Comparison of the experimental level density of ^{56}Fe with a microscopic theory. The figure is taken from Ref. [24]. Experimental data: o from counting levels; ⊥ from Γ/D_0, σ^2 rigid; — from charged-particle spectra. Theoretical calculations: — — — Seeger levels; ... Nix levels.

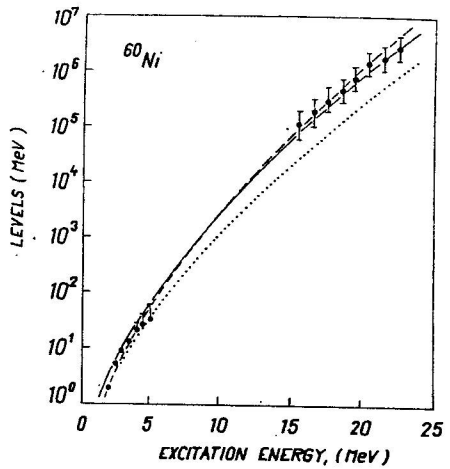

Fig. 5. Comparison of the experimental level density of ^{60}Ni, Ref. [24]. Experimental data: . from counting levels; ⊥ from Γ/D_0, σ^2 rigid; — from charged-particle spectra. Theoretical calculations: — — — Seeger levels; ... Nix levels.

Bolsterli et al. [23] applied the microscopic model in calculations of the decay width for fission as well as for neutron and gamma ray emission. However, first Behkami and Huizenga [24] and Ignatyuk et al. [25] have initiated a systematic comparison of the experimental level densities and spin cut-off factors with the microscopic theory calculations. Such comparisons were reported for Mn, Fe, Co, Ni and Cu isotopes. Behkami and Huizenga [24] used two sets of single particle levels obtained by Seeger and Perisho [26] and by Bolsterli et al. [27] in their calculations. The values of the energy gap parameters for doubly even nuclei taken from literature [28—31] were used as input data in the calculations. The resulting level densities for ^{56}Fe and ^{60}Ni are compared with the experimental data in Figs. 4 and 5. The agreement between the microscopic theory and experiment is very good. In Fig. 6 the spin cutoff parameters σ_2 extracted from angular distribution measurements [32] are compared with the values calculated from microscopic theory for ^{56}Fe. The importance of the shell structure appears in that figure in the difference of contributions from neutrons and protons. The dominance of the proton contribution σ_p^2 is connected to the large occupation probability for the $1f_{7/2}$ single particle levels in ^{56}Fe.

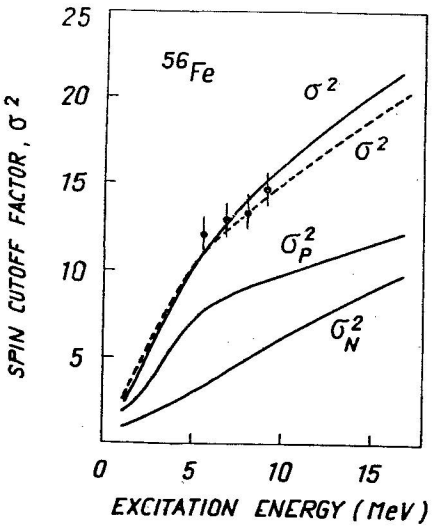

Fig. 6. Comparison of the experimental spin cut-off factor with a microscopic theory calculation. The figure is taken from Ref. [32]. ⊥ experimental; — Seeger levels; — — — Nix levels.

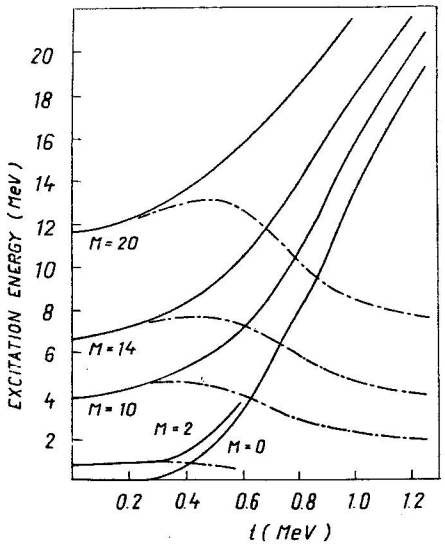

Fig. 7. The excitation energy as a function of thermodynamic temperature for different angular momentum projections M (solid lines). The dott-dashed lines represent the effective rotational energy. The thermal excitation energy corresponds to the $M = J = 0$ line.

The angular momentum dependence of the level density can be improved when the projection of the angular momentum on the quantization axis is introduced into the *BCS* Hamiltonian as an additional constant of motion [33].

In this case the entropy of the nucleus is

$$S = \ln Z - \beta E - \beta\lambda_n N_n - \beta\lambda_p N_p - \beta\omega M, \qquad (22)$$

where gas is the Lagrange multiplier which fixes the angular momentum projection M. The magnitude ω may be interpreted as an angular velocity of the rotational motion connected with the angular momentum. The grand partition function depends now not only on the single particle energies but also on the magnetic quantum numbers m_k of the single particle states.

$$\ln Z = -\beta \sum_k (\varepsilon_k - \lambda - E_k) + \sum_k \ln [1 + \exp(-\beta E_k + \beta\omega m_k)] + \qquad (23)$$

$$+ \sum_k \ln [1 + \exp(-\beta E_k - \beta\omega m_k)] - \beta\Delta^2/G.$$

It also applies to the gap equation and the equations defining the constants of motion N and E. Additionally the angular momentum projection is given by

$$M = \sum_k m_k \left[\frac{1}{1 + \exp\beta(E_k - \omega m_k)} - \frac{1}{1 + \exp\beta(E_k + \omega m_k)} \right]. \qquad (24)$$

For the nucleus we replace $\sigma^2 = \sigma_k^2 + \sigma_p^2$ by $M = M_n + M_n$. The dependence of the density of states on M is no longer analytic and the parameter σ^2 no longer appears in the calculations. In the case of the shell model scheme the calculation is complicated because of discontinuities in the above given equations for the ground state. The unknown variables Δ, λ and ω can be obtained by solving the gap equation, and the equations for N and M, for given t and G values. The angular momentum is created by breaking up pairs and by aligning the resulting quasiparticles which block the single particle levels close to the Fermi energy. It destroys the pairing correlations and causes an increase of the momentum of inertia. For angular momenta near the critical value a thermally assisted pairing can be observed [33, 34]. This is connected with the fact that at large angular momenta and low temperatures all the quasiparticles are tightly packed around the Fermi surface. An increase of temperature, instead of breaking pairs, spreads out the quasiparticles and diminishes the effect of blocking.

The above formulation takes automatically into account the yrast cut-off of the spin distribution. In Fig. 7 the excitation energy as a function of temperature is shown. The excitation energies corresponding to different $M = J$ values at zero temperature are entirely connected with the intrincisc rotation and define the yrast levels.

The model presented provides a comprehensive view of many physical quantities like the pairing energy gap, the moment of inertia, the rotational frequency or the entropy. However, some important limitations are inherent to the model connected with the existence of spurious solutions and the reliability of the phase transition effects [35].

REFERENCES

[1] Bethe H. A., Rev. Mod. Phys. *9* (1937), 69.
[2] Lang I. M. B., LeCouter J., Proc. Phys. Soc. *A 47* (1954), 585.
[3] Facchini U., Saetta-Menichella E., Energia Nucleare *16* (1968), 54.
[4] Baba H., Nucl. Phys. *A 159* (1970), 625.
[5] Gilbert A., Cameron A. C. W., Can. J. Phys. *43* (1965), 1446.
[6] Browne J. C., Newson H. W., Bilpuch E. G., Mitchell G. E., Nucl. Phys. *A 153* (1970), 481.

[7] Lindstrom D. P., Newson H. W., Bilpuch E. G., Mitchell G. E., Nucl. Phys. *A 168* (1971), 37.
[8] Blatt J. M., Biedenharn L. C., Rev. Mod. Phys. *24* (1952), 258.
[9] Lu C. C., Vaz L. C., Huizenga J. R., Nucl. Phys. *A 190* (1972), 229.
[10] Ericson T., Advan. Phys. *9* (1960), 425.
[11] Huizenga J. R., Vonach H. K., Karsanos A. A., Gorski A. J., Stephan C. J., Phys. Rev. *182* (1969), 1149.
[12] Lang D. W., LeCounter K. J., Nucl. Phys. *14* (1959), 24.
[13] Katsanos A. H., *Argonne National Laboratory Report*, ANL-7289, 1967.
[14] Gadioli E., Iori I., Marini A., Sansoni M., Nuovo Cimento *44 B* (1966), 338.
[15] Bloch C., Phys. Rev. *93* (1954), 1094.
[16] Rosenzweig N., Phys. Rev. *105* (1957), 108.
[17] Hilman M., Grover J. R., Phys. Rev. *185* (1969), 1303.
[18] Malov L. A., Soloviev V. G., Vorronov V. V., Nucl. Phys. *A 224* (1974), 396.
[19] Soloviev V. G., Stoyanov Ch., Vdovin A. I., Nucl. Phys. *A 224* (1974), 411.
[20] Sano M., Yamasaki S., Progr. Theor. Phys. *29* (1963), 277.
[21] Decowski P., Grochulski W., Marcinkowski A., Nucl. Phys. *A 194* (1972),
[22] Decowski P., Grochulski W., Marcinkowski A., Siwek K., Wilhelmi Z., Nucl. Phys. *A 110* (1968), 129.
[23] Britt H. C., Bolsterli M., Nix J. R., Norton J. L., Phys. Rev. *C 7* (1973), 801.
[24] Behkami A. N., Huizenga J. R., Nucl. Phys. *A 217* (1973), 78.
[25] Ignatyuk A. B., Sokolov J. W., Szubin I. N., *Zentr. Kernf. Dresden Rep.* Zfk-271 (1974), 21.
[26] Seeger P. A., Perisko R. C., *Los Alamos Scientific Laboratory Rep.* LA 3751 (1957).
[27] Bolsterli M., Fiset E. O., Nix J. R., Norton J. L., Phys. Rev. *C 5* (1972), 1050.
[28] Cameron A. G. W., Can. J. Phys. *34* (1956), 804.
[29] Nemirowski P. E., Adamchuk Yu. V., Nucl. Phys. *39* (1962), 551.
[30] Gilbert A., Cameron A. G. W., Can. J. Phys. *43* (1965), 1446.
[31] Kümmel H., Mattauch J. H. E., Thiele W., Wapstra A. H., Nucl. Phys. *81* (1966), 129.
[32] Lu C. C., Vaz L. C., Huizenga J. R., Nucl. Phys. *A 97* (1972), 321.
[33] Kammuri T., Progr. Theor. Phys. *31* (1964), 595.
[34] Moretto L. G., Nucl. Phys. *A 216* (1973), 1.
[35] Ignatyuk A. W., Sokolow I. W., *Zentr. Kernf. Dresden, ZfK-271* (1974), 7.

Received October 10th, 1975